Carrier Generation Lifetimes in 4H-SiC MOS Capacitors

Matthew J. Marinella, *Member, IEEE*, Dieter K. Schroder, *Life Fellow, IEEE*, Gilyong Chung, Mark J. Loboda, *Senior Member, IEEE*, Tamara Isaacs-Smith, and John R. Williams, *Member, IEEE*

***Abstract*—The field of SiC electronics has progressed rapidly in recent years, but certain electronic properties remain poorly understood. For example, a consensus has not been reached as to the specific point defects which limit minority carrier recombination, and little is known about defects which limit generation lifetimes. This paper investigates generation lifetimes using the pulsed MOS capacitor technique and compares the results with defect densities, recombination lifetimes, and Schottky diode characteristics in the same material for the first time. Carrier generation lifetimes in 4H-SiC epilayers range from less than 1 ns to approximately 1 μs and depend strongly on measurement conditions and data interpretation. They are limited by dislocations only at densities higher than 10^6 cm^{-2}. The only point defect that is theoretically capable of limiting generation lifetime to the levels currently observed in 4H-SiC is $EH6/7$. However, this defect cannot account for the case where generation lifetimes are lower than recombination lifetimes in the same area. This is not seen in silicon and seems to be inconsistent with theory. Possible reasons for these perplexing results are discussed, and it is attempted to form a framework with which further understanding of the significance of carrier generation lifetime measurements in SiC can be achieved.**

***Index Terms*—Carrier generation, carrier lifetimes, carrier recombination, MOS capacitors (MOS-Cs), semiconductor device measurements, silicon compounds.**

I. Introduction

SILICON CARBIDE (SiC) is a long standing candidate to replace silicon in device applications requiring high temperature, high power, and extreme environments. The wide bandgap permits theoretical operation at temperatures in excess of 600 °C, and the high electric breakdown field allows the fabrication of devices with a theoretical power efficiency two orders of magnitude better than silicon devices. While much progress has been made, commercial devices are not available on a wide scale, in part, because some of the basic semiconducting properties of SiC are still not fully understood. One example of this is the lack of a consensus as to the defects which limit carrier recombination and generation lifetimes.

Carrier recombination in 4H silicon carbide is a topic of current ongoing research [1], [2]. It is important to understand and control recombination lifetime (τ_r) in order to produce bipolar devices with uniform electrical parameters. Klein *et al.* have given strong evidence that the intrinsic $Z1/2$ defect limits the recombination lifetime [1]. Other work has suggested that both the $Z1/2$ and $EH6/7$ defects are the limiters [2].

Much less attention has been given to carrier generation and generation lifetimes. Generation lifetime (τ_g) is a significant property of a semiconducting material because it determines the reverse-bias leakage current of a p-n junction. Since excessive generation current in a reverse-biased junction leads to a high reverse-bias leakage current and can degrade the breakdown voltage, it is usually desirable to have long generation lifetimes. Short generation lifetimes also may indicate the presence of defects which adversely affect other device properties such as the oxide integrity of MOS devices.

This paper makes use of the pulsed MOS capacitor (MOS-C) technique to measure the carrier generation lifetimes of a large number of 4H-SiC/SiO$_2$ MOS-Cs. Furthermore, in order to better understand the significance of the resulting generation lifetimes, Schottky diode properties and recombination lifetimes in the same physical location as the MOS-Cs were also characterized. During the application of the pulsed MOS-C technique to the SiC MOS-C, a number of nonidealities were uncovered, which had the potential to affect the generation lifetimes resulting from this method. The physical causes and potential effects of these nonidealities on the data are discussed in order to avoid future misinterpretations of pulsed SiC MOS-C measurements. Finally, it is noted that the ratio of generation to recombination lifetime in SiC is much lower than that observed in silicon, and the reasons for this perplexing result are discussed.

II. Generation and Recombination Theory

Since this paper is concerned with generation and recombination lifetimes in silicon carbide, it is useful to briefly review the kinetics of these processes. The following discussion outlines the important points relevant to the results which follow; a more complete treatment can be found in the common semiconductor texts such as [3] and [4] or in the detailed work by Sah [5].

Manuscript received September 9, 2009; revised February 12, 2010; accepted May 7, 2010. Date of current version July 23, 2010. This work was supported by the ONR Contract N00014-05-C-0324 (with Dr. Paul Maki as the Program Officer). The review of this paper was arranged by Editor S. Bandyopadhyay.

M. J. Marinella was with the Department of Electrical Engineering and the Center for Solid State Electronics Research, Arizona State University, Tempe, AZ 85287-5706 USA. He is now with the Radiation Hardened CMOS Technology Department, Sandia National Laboratories, Albuquerque, NM 87185-1084 USA (e-mail: mmarine@sandia.gov).

D. K. Schroder is with the Department of Electrical Engineering and the Center for Solid State Electronics Research, Arizona State University, Tempe, AZ 85287-5706 USA.

G. Chung and M. J. Loboda are with Dow Corning Compound Semiconductor Solutions, LLC, Midland, MI 48611 USA.

T. Isaacs-Smith and J. R. Williams are with the Physics Department, Auburn University, Auburn, AL 36849 USA.

Color versions of one or more of the figures in this paper are available online at http://ieeexplore.ieee.org.

Digital Object Identifier 10.1109/TED.2010.2051196

0018-9383/$26.00 © 2010 IEEE

Authorized licensed use limited to: Arizona State University. Downloaded on August 05,2010 at 17:03:41 UTC from IEEE Xplore. Restrictions apply.

Generation occurs when there is a lack of carriers, or $np < n_i^2$, at a rate G characterized by the generation lifetime $\tau_g \equiv n_i/G$. Carriers attempt to restore equilibrium as a result of three different fundamental processes: optical generation, impact ionization, and through thermal emission of electrons and holes by energy levels within the bandgap created by defects. Since optical generation and impact ionization do not play a significant role in our results, the remainder of this discussion will focus on thermal generation through defects. It is possible that significant densities of several different kinds of defects exist within a material, each acting as an independent generation source. Examples are uniformly distributed point defects (such as the $Z1/2$ and $EH6/7$ in SiC), surface/interface states, as well as levels due to dislocations. Since generation sources act in parallel, the generation lifetimes from different sources are combined to find the total generation lifetime as

$$\frac{1}{\tau_g} = \frac{1}{\tau_{g,\text{bulk defect}-1}} + \frac{1}{\tau_{g,\text{bulk defect}-2}} + \frac{1}{\tau_{g,\text{surface}}} + \frac{1}{\tau_{g,\text{dislocations}}}. \quad (1)$$

The inverse process, recombination, occurs when excess carriers are present $(np > n_i^2)$ at a rate R characterized by the recombination lifetime $\tau_r \equiv \Delta n/R$, where Δn is the excess minority carrier concentration. All generation mechanisms have equivalent recombination mechanisms.

A. Shockley–Read–Hall Theory

Carrier generation and recombination rates through single-level traps are given by [6], [7]

$$R = -G = \frac{np - n_i^2}{\tau_p(n + n_1) + \tau_n(p + p_1)}. \quad (2)$$

The high-level injection recombination lifetime is given by [8]:

$$\tau_r = \tau_p + \tau_n, \qquad (n \approx p) \quad (3)$$

and the low-level injection recombination lifetime by

$$\tau_r = \tau_p \ (n \gg p, n\text{-type substrate})$$
$$\tau_r = \tau_n \ (p \gg n, p\text{-type substrate}). \quad (4)$$

The generation lifetime τ_g is given by

$$\tau_g = \tau_p e^{\frac{E_T - E_i}{kT}} + \tau_n e^{-\frac{E_T - E_i}{kT}} \quad (5)$$

which can be simplified to

$$\tau_g \approx 2\tau_r \sqrt{\frac{\sigma_n}{\sigma_p}} \cosh\left(\frac{E_T - E_i}{kT}\right) \quad (6)$$

and if the cross sections are equal, this becomes

$$\tau_g \approx \tau_r e^{\frac{|E_T - E_i|}{kT}} (\sigma_n = \sigma_p). \quad (7)$$

Equation (7) states that, as long as the capture cross sections are approximately equal, the ratio of the generation to recombination lifetimes is determined mainly by $|E_T - E_i|$ and a given capture cross section.

B. Surface Effects

Generation and recombination lifetimes are affected by surface states. Surface effects are generally characterized by a velocity rather than a characteristic time. In the case of a uniform density of surface states (D_{it}), surface generation in a depletion region, such as a reverse-biased p-n junction or MOS-C in depletion, is related to the number of interface traps N_{it} through [9]:

$$s_g = \sigma v_{\text{th}} N_{\text{it}} \quad (8)$$

where σ_s is the capture cross section of the surface state. By integrating over energy, the relation to D_{it} is found to be [9]

$$s_g = \sigma v_{\text{th}} (\pi k T D_{\text{it}}). \quad (9)$$

Unfortunately, it is usually not possible to calculate s_g from D_{it} with this simple equation, because D_{it} is not uniform across the bandgap; it is often much higher near the band edges at energies which do not contribute strongly to emission. Furthermore, the values of σ_s are often not well known and depend on the specific measurement technique. However we do know, at least qualitatively, that surface generation depends on the quality of the interface—which is usually poor for SiC/SiO_2 interfaces. Clearly, one cannot neglect the effect that surface generation has on lifetime measurements.

The generation lifetimes presented in this paper are determined with a Zerbst plot. The two values extracted from a Zerbst plot are the effective bulk lifetime $\tau_{g,\text{eff}}$ and the effective surface generation velocity $s_{g,\text{eff}}$ [4]. Each component is influenced by multiple generation mechanisms. The effective generation lifetime is made up of components which depend on the width of the space-charge region (SCR), and is given by [4]:

$$\tau_{g,\text{eff}} = \left(\frac{1}{\tau_g} + \frac{2s_g}{r}\right)^{-1} \quad (10)$$

where τ_g is the true bulk lifetime in the SCR, s_g is the surface generation velocity which is lateral to, but not under, the gate area, and r is the device radius. $s_{g,\text{eff}}$ is influenced by the generation processes which do not depend on the SCR width, i.e., the surface generation directly under the gate and the bulk generation outside the SCR, given by (assuming an n-type bulk)

$$s_{g,\text{eff}} = s_0 + \frac{q n_i D_p}{N_D L_p} \quad (11)$$

where s_0 is the surface generation directly under the gate, L_p is the minority carrier diffusion length in the bulk, and D_p is the diffusion coefficient of holes. Hence, a high surface generation velocity not only increases the effective surface generation velocity but also reduces the effective generation lifetime $\tau_{g,\text{eff}}$, as shown in Fig. 1 (using the properties of a typical 4H-SiC MOS-C). In this device, surface generation velocity higher than about 10^4 cm/s considerably decreases the effective bulk lifetime.

Authorized licensed use limited to: Arizona State University. Downloaded on August 05,2010 at 17:03:41 UTC from IEEE Xplore. Restrictions apply.

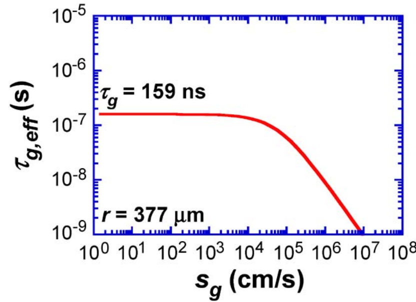

Fig. 1. Effective bulk generation lifetime versus surface generation velocity (10) for a 4H-SiC device. s_g is the surface generation which is lateral to, but not under, the gate area.

Surface effects also play a role in recombination lifetimes. The recombination lifetimes presented in this paper are measured optically. When excess carriers are optically induced near the sample surface, they clearly can recombine at that surface. If the interface between an epitaxial layer of thickness t and the substrate is within the minority carrier diffusion length from the point where the carriers are injected, it will play a role also. The effective lifetime is given from surface and bulk contributions as

$$\tau_{r,\mathrm{eff}} = \frac{\tau_{r,\mathrm{bulk}}}{1 + \tau_{r,\mathrm{bulk}}/\tau_s} \tag{12}$$

where the surface recombination lifetime (τ_s) is given by $\tau_s \approx t/2s_r$ when surface recombination is low (where s_r is the surface recombination velocity), and $\tau_s \approx t^2/\pi^2 D_p$ when it is high [8]. When a measurement is dominated by surface recombination, the bulk component makes up a small part of the effective lifetime, since $\tau_{r,\mathrm{bulk}} \gg \tau_s$.

C. Dislocations

Dislocations are present in SiC epilayers and have been shown to affect carrier lifetimes. The dislocation space-charge theory was originally derived by Morrison [10] based on the dislocation space-charge model of Read [11]. The effect of dislocations on the recombination lifetime was first studied experimentally by McKelvey [12] and Wertheim and Pearson [13] in Ge samples; it was found that, when dislocation densities are higher than about 10^4 cm^{-2}, lifetime and dislocation density ρ_D are related by

$$\tau_r = \frac{c}{\rho_D} \tag{13}$$

where c is a constant on the order of unity (in the range of 0.7–2.5 s/cm^2 for Ge). A recent work indicates that SiC follows a similar rule; the recombination lifetime is limited by dislocations above a threshold density of about 10^6 cm^{-2} [14].

III. Deep Levels and Carrier Lifetimes in 4H-SiC

The energy levels of the most important two intrinsic point defects suspected to play a role in the recombination lifetimes of 4H-SiC $Z1/2$ and $EH6/7$ are summarized pictorially in Fig. 2. The $Z1/2$ defect has an energy level of about 0.65 eV below the conduction band, making it an unlikely candidate

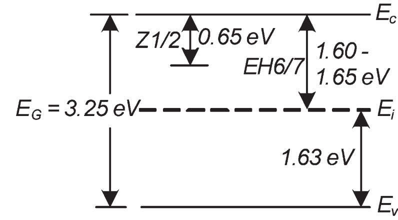

Fig. 2. Deep levels in 4H-SiC, which are suspected of limiting recombination lifetimes. Data from [2] and [16].

to limit generation lifetime, due to the large difference in energy from E_i. Although it has not yet been proven, it is suspected that this defect results from the silicon and carbon divacancy. The electron capture cross section for the $Z1/2$ defect ranges from 3×10^{-15} to 2×10^{-14} cm^{-2} [2] and about 2×10^{-14} cm^{-2} for holes [15]. The $EH6/7$ defect is near the center of the band (at about 1.60 eV), and has an electron capture cross section in the range of 2×10^{-13} to 9×10^{-12} cm^{-2} [2], [16]. The capture cross section for holes has not been reported for the $EH6/7$ defect. The origin of this defect is also unknown, but the carbon vacancy is strongly suspected to be the cause [2].

The results of several recombination lifetime studies are summarized in Table I. A large number of optical recombination lifetime measurement data have been reported, with recombination lifetime values ranging from several nanoseconds to a few microseconds. Using photoluminescence decay (PLD), Kordina *et al.* found lifetime to be the longest near the center, where the density of structural defects is the lowest [17]. Zhang *et al.* and Tawara *et al.* find an inverse correlation between τ_r and the densities of $Z1/2$ and $EH6/7$ defects [2], [18]. Danno *et al.* used microwave photoconductance decay (MPCD) to map the distribution of $Z1/2$ defects and correlate densities of this defect with recombination lifetime [19]. Galeckas *et al.* used depth-resolved transient absorption (TA) to evaluate the effects of processing on τ_r [20]. Chung *et al.* found decreased levels of the $Z1/2$ defect and increased recombination lifetimes in chlorosilane-based epilayers, suggesting that $Z1/2$ is not a dominant recombination lifetime limiter when this chemistry is used [21]. Mori *et al.* found that lifetime *increased* near structural defects, possibly due to trapping [22]. Both Kordina *et al.* and Tawara *et al.* reported an increase in recombination lifetime at higher temperatures [17], [18].

There are also several reports on the electrical characterization of recombination lifetimes. Kimoto *et al.* used reverse recovery (RR) to measure τ_r in diodes and found that it was limited by strong perimeter recombination [23]. Cochrane *et al.* used the results of spin-dependent recombination (SDR) measurements to conclude that a midlevel defect such as $EH6/7$ limits the current gain in bipolar junction transistors [24].

When it is reported, surface recombination velocity is often high (on the order of $10^3 - 10^5$ cm/s), suggesting that it affects the reported bulk lifetimes in many cases. Klein *et al.* carefully take into account the effects of surface recombination using substrates with different epilayer thicknesses [15]. They are then able to calculate the approximate surface recombination velocity of 2500 cm/s, which includes the true surface and the interface between the epilayer and substrate. After accounting for this, they calculate the true bulk lifetimes and compare these

Authorized licensed use limited to: Arizona State University. Downloaded on August 05,2010 at 17:03:41 UTC from IEEE Xplore. Restrictions apply.

TABLE I
PARTIAL SUMMARY OF KEY RECOMBINATION LIFETIME DATA IN SiC

Author	Year	PT	Method	τ_{max} (μs)	τ_{min} (μs)	s_r (cm/s)	Main Conclusions	Ref
Chung	2007	4H	MPCD	5	2	-	Chlorosilane based epilayers have fewer Z1/2 defects and increased τ_r	21
Cochrane	2007	4H	SDR	-	-	-	Vacancy (such as *EH6/7*) limits current gain in BJT	24
Danno	2007	4H	MPCD	2.3	0.07	-	*Z1/2* affects τ_r when $N_T > 10^{13}$ cm^{-2}	19
Klein	2006	4H	PLD	≈ 0.5	≈ 0.25	2500	*Z1/2* are τ_r limiters	15
Jenny	2006	4H	MPCD	> 3	0.01	-	τ_r increased by annealing	25
Mori	2005	4H	MPCD	≈ 0.06	≈ 0.02	-	τ_r *increases* with increased structural defect densities	22
Tawara	2004	4H	MPCD, PLD	1.4	0.26	-	Correlates *EH6/7*, *Z1/2*, and *D1* center with τ_r; τ_r increases with T	18
Zhang	2003	4H	PLD	0.3	0.05	-	*EH6/7* and *Z1/2* centers decrease τ_r	2
Galeckas	2001	4H/6H	TA	≈ 0.9	0.02	5×10^3-5×10^5	Processing reduces τ_r; s_r dominates in layers thinner than 100 μm	20
Kimoto	1999	4H/6H	RR	≈ 0.3	-	≈10^4	τ_r limited by perimeter recombination	23
Kordina	1996	4H/6H	PLD	2.1	0.11	-	Highest τ_r near center of wafer; τ_r increases with T	17

with the density of various defects. A strong correlation is found between lifetime and $Z1/2$ densities, whereas no correlation with the $EH6/7$ densities and lifetime is found. This appears to provide evidence that, in this case, recombination lifetime is limited by the $Z1/2$ defect.

Only a handful of papers exist which evaluate the generation lifetime in SiC. The only pulsed MOS-C generation lifetimes quoted in the literature of which we are aware are 30 ns at 275 °C [26] and between 19 and 45 ns at 334 °C [27], obtained using similar 6H n-type samples from Cree. The work of Wang *et al.* uses an approach which makes use of an n-p-n device rather than the pulsed MOS-C and extracts generation lifetimes of approximately 50 ns [28]. This work is significant because it uses a structure that is less susceptible to surface generation than the MOS-C and systematically considers and removes surface effects from the results.

IV. EXPERIMENTAL DETAILS

Dow Corning n-type 4H-SiC research grade material was used with 10–20-μm chlorosilane-chemistry-based epilayers with an approximate nitrogen doping density of 10^{16} cm^{-3}. To form MOS-C, small samples (about 1 cm^2) were oxidized on the Si face and annealed in NO, and Mo/Au gates were deposited using photolithography, as described in [29]. The samples had oxide thicknesses ranging from 40 to 70 nm. We measured generation lifetimes and leakage currents on seven samples using the pulsed MOS-C measurement technique at 400 °C, as described in detail in [30]. Low gate voltages of -1 to -5 V were used to minimize the effects of gate leakage and field-dependent generation. Following the generation lifetime measurements, PLD recombination measurements were made in the same locations as the generation lifetime measurements. All PLD measurements were made at the Naval Research Laboratory using the procedure described in [1].

After the generation and recombination lifetimes had been measured, the oxide was stripped, and three samples were etched with potassium hydroxide (KOH) to determine common dislocation densities associated with the region occupied by each MOS-C. However, two of the samples (prior to the KOH etch) had Schottky barrier diodes (SBDs) fabricated in the same location and with the same diameter as the MOS-C. To create these diodes, two samples were reactive ion etched using the Mo/Au capacitors as the mask in order to create mesas around the MOS-C structures. Then, the MOS-C metal and oxide were wet etched, and $NiV_{7\%}$ Schottky gates were deposited and etched with the same photolithographic mask as the MOS-C, using the mesas for alignment. These samples are referred to hereinafter as DOW1 and DOW2. As a control, SBDs were created on a fresh sample from the same wafers as the other SBD/MOS-C samples. These diodes were formed by depositing the same $NiV_{7\%}$ alloy and etching the metal with the same photolithographic mask. Finally, mesas were fabricated around the diodes on the fresh sample using RIE. This sample is referred to hereinafter as DOW4.

V. RESULTS AND DISCUSSION

A. *Effect of Dislocations and Wafer Growth Angle on Generation Lifetime*

Generation lifetimes were measured on several samples with maximum dislocation densities ranging from 10^3 to 10^6 cm^{-2}. For these samples, the generation lifetimes were compared with the number of threading edge dislocations, screw dislocations, and basal plane dislocations on the surface of each device. This comparison is shown in Fig. 3 for each type: threading edge dislocations [Fig. 3(a)], screw dislocations [Fig. 3(b)], and basal plane dislocations [Fig. 3(c)]. The results show the generation lifetime to be poorly correlated

Authorized licensed use limited to: Arizona State University. Downloaded on August 05,2010 at 17:03:41 UTC from IEEE Xplore. Restrictions apply.

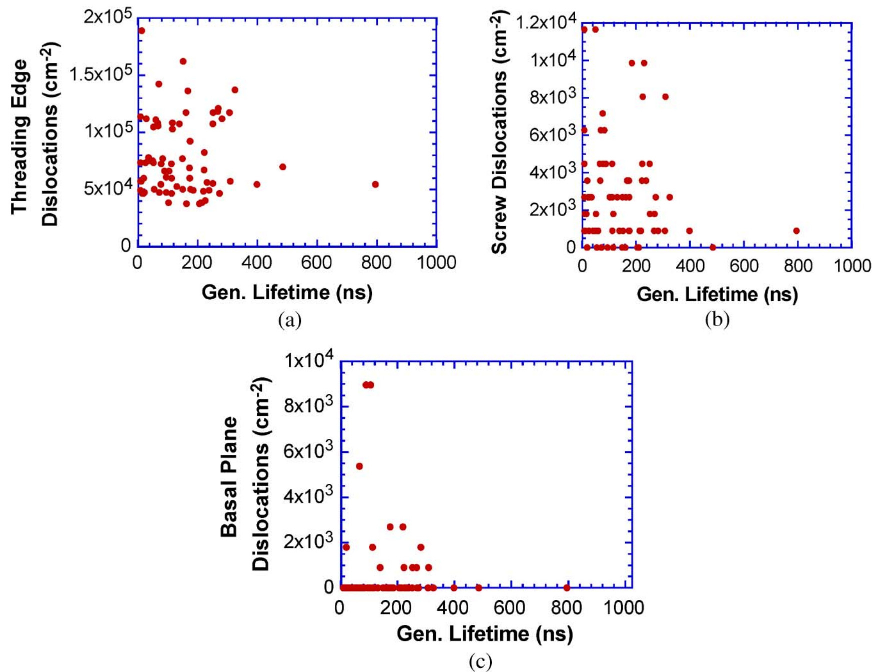

Fig. 3. Comparison of dislocation densities versus generation lifetimes for (a) threading edge dislocations, (b) screw dislocations, and (c) basal plane dislocations.

TABLE II
SUMMARY OF AVERAGE MOS-C GENERATION LIFETIMES FOR DIFFERENT WAFER LOCATIONS

Location	$\tau_{g,eff}$ (ns)	Dislocation Density (cm^{-2})
Center	705	$2x10^4$
Between edge and center	557	$4x10^4$
Edge	240	$3x10^6$

with dislocation densities, demonstrating that, at dislocation densities below about 10^6 cm^{-2}, the generation lifetime is not limited by these dislocations. To further study the effect of dislocations, MOS-Cs were fabricated on samples taken from the center, edge, and an intermediate spot on a wafer. In this case, the defect densities on each sample (45 devices per sample) were averaged to provide a macroscopic comparison. The summary of dislocation densities and average generation lifetimes for each location is given in Table II. Each average generation lifetime represents values obtained from 45 devices. This suggests that, on a macroscopic level, generation lifetime is limited by dislocations when the density is higher than about 10^6 cm^{-2}. Birefringence maps of the three samples (Fig. 4) confirm the high defect densities in the sample taken from near the edge of the wafer, where the generation lifetime is lowest. It should be noted that, within the sample taken near the edge, there was not a strong correlation between dislocation densities on individual devices (as counted in etch pits) and generation lifetimes of these devices. This is because, on this sample, the etch pit counts were only approximate due to the large number of long grain boundaries, which would often render individual etch pits difficult to distinguish.

The samples discussed thus far were grown at an angle of 8° from the *c*-axis. An additional sample grown at 4° was used to observe the effect of the growth angle of the epitaxial layer on generation lifetime. The average lifetime of this sample was about 700 ns, indicating that there is not a significant difference in average generation lifetimes for 4° and 8° of axis epilayers.

High-resolution recombination maps were measured using PLD, giving data for the same locations as the MOS-C. The recombination lifetimes ranged from 500 to 700 ns and did not correlate well with the generation lifetimes. On samples where extended defects were not present, it is possible that τ_r was limited by recombination at the interface between the epilayer and substrate, due to the relatively thin epilayers (20 μm). This may provide an explanation as to why τ_r did not correlate well with τ_g. However, this does not necessarily explain why, in this paper, as well as in all of the literature, the recombination lifetime is always longer or approximately equal to the generation lifetime, as discussed in Section V-D.

B. Comparison With Schottky Diodes

The SiC SBD has been the subject of numerous studies [31]–[33]. This device is similar to the MOS-C in the sense that it is very sensitive to conditions at or near the surface of the epilayer. It was therefore of interest to investigate whether the same defects which play a role in the generation lifetimes affect the Schottky characteristics. In order to study this, three MOS-C samples (135 devices) were used; generation lifetime values had been measured for all of the devices. Schottky diodes were fabricated in the exact locations where the original capacitors were located as described in Section IV.

The Schottky diode I–V curves were then measured, and the results were analyzed using a parallel diode model based on that described by Skromme *et al.* [32]. The parallel diode model is used to describe I–V curves with a "kink" characteristic of a defect. These curves result in two barrier heights, the lower of which represents the current through the defective area and the

Authorized licensed use limited to: Arizona State University. Downloaded on August 05,2010 at 17:03:41 UTC from IEEE Xplore. Restrictions apply.

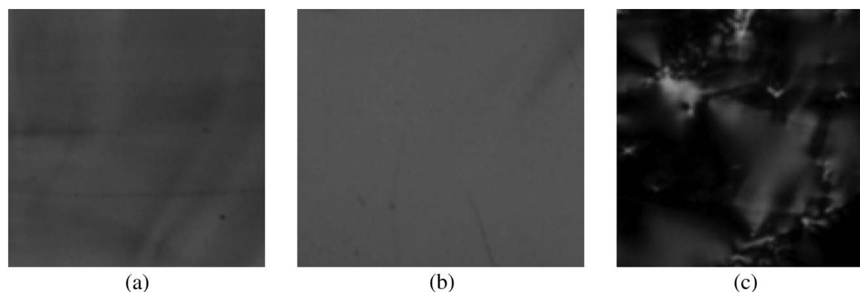

Fig. 4. Birefringence maps of the samples from (a) the center of the wafer, (b) between the edge and center, and (c) near the edge of the wafer.

TABLE III
SUMMARY OF AVERAGE MOS-C GENERATION LIFETIMES, SCHOTTKY BARRIER HEIGHTS, AND IDEALITY FACTORS FOR DEVICES ON SAMPLE DOW1

DOW1	N	$\tau_{g,eff}$ (ns)	φ_{B1-IV} (eV)	n_1	φ_{B-CV} (eV)
All Devices	**45**	**705**	**1.162**	**1.400**	**1.766**
Normal	38	756	1.200	1.274	1.760
Two Diode (D1)			1.164	1.568	
Two Diode (D2)	4	375	0.966	1.471	1.807
Ohmic (φ_B<1.0eV)	3	426	0.689	2.727	1.769

TABLE IV
SUMMARY OF AVERAGE MOS-C GENERATION LIFETIMES, SCHOTTKY BARRIER HEIGHTS, AND IDEALITY FACTORS FOR DEVICES ON SAMPLE DOW2

DOW2	N	$\tau_{g,eff}$ (ns)	I_{ox} (fA)	φ_{B1-IV} (eV)	n_1	φ_{B-CV} (eV)
All Devices	**45**	**557**	**588**	**1.147**	**1.86**	**1.646**
Normal	29	705	560	1.202	1.353	1.646
Two Diode (D1)				1.027	2.103	
Two Diode (D2)	14	243	663	0.673	1.930	1.645
Ohmic (φ_B<1.0eV)	2	165*	NA	0.613	7.393	1.675

* Generation lifetime data available from only one device.

higher represents the current through the rest of the device. In addition, barrier heights were extracted from the C–V curve, using the standard technique described in [4].

Summaries of the data obtained from the MOS-C and Schottky diode analysis for two samples are given in Tables III and IV. The devices are divided into three categories based on the I–V behavior of the Schottky diodes. It should be noted that all of the ideality factors are higher than one would expect for a typical SiC SBD, and all of the barrier heights are low, which can be attributed to the previous oxidation and formation and testing of MOS-C. The "normal" group includes devices which exhibit ideal forward-biased Schottky diode I–V behavior. The I–V curves of some of the normal devices exhibited slight abnormalities such as current spikes, most likely due to contact problems. These abnormalities were not considered in the analysis. The devices within the "two-diode" group are those with characteristics matching the parallel diode model. The "D1" values are extracted from the ideal portion of the I–V curve and the "D2" values from the nonideal portion of this curve. Finally, the "ohmic" group consists of devices which have forward-biased I–V curves that did not exhibit a rectifying behavior (these curves were nearly ohmic). In addition, there was no observable inflection point in the I–V curve for the ohmic devices, which negates the use of the parallel conductor model or the shunt resistor model. On both samples, the barrier heights obtained from the C–V technique were reasonably constant within each sample.

Tables III and IV show that, in both cases, a significant difference in generation lifetime exists between devices which exhibit normal I–V behavior and those which do not. This suggests that, on average, the defects that affect forward-biased Schottky diode characteristics also affect the generation lifetime. However, some devices do not follow this trend (i.e., a well-behaved Schottky diode had a very short generation lifetime or vice versa); the reason for this is not clear at this time.

In addition to studying the behavior of devices on individual samples, insight is gained from a comparison of the average behaviors of all devices on a particular sample. DOW1 was taken from the prime location near the center of the wafer, where material quality was highest. DOW2 and DOW4 were taken from adjacent spots closer to the wafer edge, where the material quality is known to be lower. DOW1 and DOW2 were oxidized and originally contained the MOS-C structures used to measure generation lifetime. DOW4 was a fresh sample only used in the Schottky diode measurements.

The results of the Schottky diode analysis are summarized in Table V. As expected from the location on the original wafer, DOW1 generally had higher average I–V barrier heights and lower average ideality factors than DOW2. The fresh sample DOW4 had better characteristics than either of the previously oxidized samples DOW1 and DOW2. For example, DOW2 had 16 diodes which followed either the two-diode or ohmic models, whereas only two were found on DOW4. It is interesting to note that the prime sample, which was oxidized (DOW1),

Authorized licensed use limited to: Arizona State University. Downloaded on August 05,2010 at 17:03:41 UTC from IEEE Xplore. Restrictions apply.

TABLE V
COMPARISON OF SAMPLES DOW1 AND DOW2 (PREVIOUSLY OXIDIZED) AND DOW4 (FRESH SAMPLE)

		DOW1		DOW2		DOW4	
No. Devices		**45**	**100%**	**45**	**100%**	**45**	**100%**
No. Devices with Schottky Type:	Typical	38	84%	29	64%	42	93%
	Two Diode	4	9%	14	31%	2	4%
	Ohmic	3	7%	2	4%	0	0%
Avg. IV Barrier Height (eV)		1.162		1.147		1.203	
Avg. IV Ideality		1.400		1.855		1.192	
Avg. CV Barrier Height (eV)		1.766		1.646		1.888	
Avg. Generation Lifetime (ns)		705		557		NA	

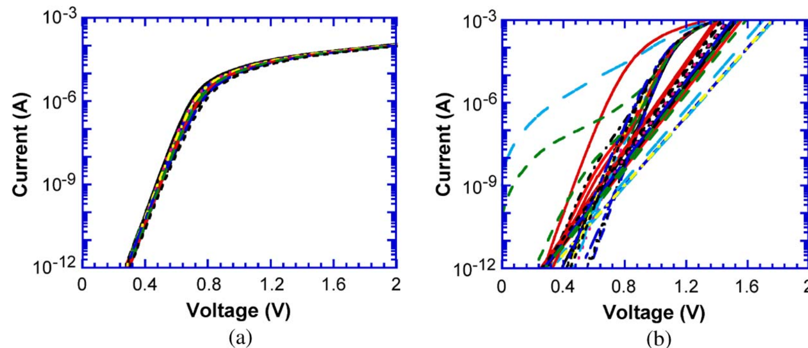

Fig. 5. Forward-biased I–V curves for Schottky diodes fabricated on adjacent spots on a wafer for (a) a fresh (unoxidized) sample and (b) a previously oxidized sample.

had significantly lower performing SBDs than the edge sample, which was not oxidized. This suggests that the degradation of the material quality near the surface due to oxidation is greater than the intrinsic degradation suffered by material near the edge of the wafer. The damage of the surface due to oxidation of two samples from the same location is made clear by the forward-biased I–V curves of DOW4 (fresh sample) and DOW2 (previously oxidized) and which are shown in Fig. 5(a) and (b), respectively. The I–V curves of the fresh sample are very uniform and show few "kinks" [Fig. 5(a)], whereas those from the previously oxidized sample are very scattered and show a number of devices which follow the two-diode model [Fig. 5(b)]. Clearly, it is possible that the oxidation damage itself may be one of the factors which limits the generation lifetime obtained from the pulsed MOS-C.

The barrier heights obtained from the C–V data follow a similar trend, with the fresh sample having a higher average barrier height than either of the previously oxidized samples. However, the C–V barrier height is thought to be lowered by 3C inclusions near the surface and not by morphological defects at the surface [34]. Our data indicate that the oxidized samples had a higher density of 3C lamellae than the fresh sample, with the sample closer to the wafer edge having a higher density of stacking faults. This is possible, as stacking faults are known to arise from oxidation [35]. However, the data do not indicate that these stacking faults significantly affected the generation lifetimes.

C. *Significance of Generation Lifetime Results*

A perplexing result of the current study was that the generation lifetimes of individual MOS-C varied as much as three orders of magnitude in a 1-cm^2 sample. Thus, clearly, these measurements are strongly affected by microscopic properties of the underlying material, interface, or oxide. However, it is not clear if these measurements indicate true bulk generation lifetimes and surface generation or if they are dictated by other phenomena such as field-enhanced emission. Therefore, it is useful to more deeply discuss the details of the pulsed MOS-C as applied in these experiments. The impact of two important nonidealities, negative-bias temperature instability (NBTI) and gate oxide leakage current, is described in detail, as they relate to the deep depletion SiC/SiO_2 MOS-C in [29] and [30], respectively. NBTI is significant in the SiC pulsed MOS-C and is discussed in the next section. Furthermore, since the measurements take place at elevated temperatures, even basic problems such as mobile ions should be taken into account in the measurement sequence [27], [30]. However, first, we consider an important factor which is observed in the Si/SiO_2 pulsed MOS-C: field-enhanced emission.

The effect of field-enhanced emission on the nonequilibrium Si/SiO_2 MOS-C was first considered by Calzolari, and it is described in detail in [36]. When present, this effect results in a reduction of the emission time constant (τ_e) from $R-G$ centers under high electric fields. The reduction of τ_e in the presence of high electric fields is due to the Poole–Frenkel effect. Fig. 6 shows this concept as it applies to the band diagram of a pulsed MOS-C. High electric fields lower the barrier height by an energy ΔE_T, increasing the emission rate. To further complicate matters, the electric field in the semiconductor is constantly changing during the recovery from deep depletion. It has been suggested by Calzolari *et al.* that field dependence causes the sharp increase of the slope often observed on the right side of the Zerbst plot [36]. The right side of the Zerbst plot represents

Authorized licensed use limited to: Arizona State University. Downloaded on August 05,2010 at 17:03:41 UTC from IEEE Xplore. Restrictions apply.

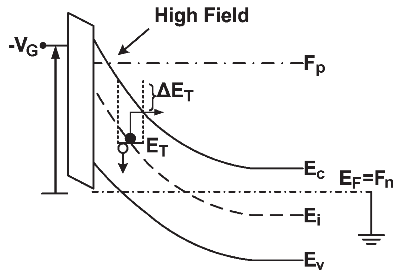

Fig. 6. Illustration of the Poole–Frenkel effect in the pulsed MOS-C.

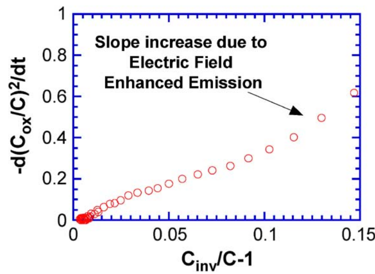

Fig. 7. Illustration of electric-field-enhanced generation commonly observed in Zerbst plots.

the beginning of the pulsed MOS-C measurement, when the electric field is the highest directly below the gate, and thus, the field-enhanced emission is highest. An example of this sharp increase in slope is shown in Fig. 7. Field-enhanced generation depends on the particular defect that dominates the generation, which may be the reason that some devices exhibit field dependence whereas other nearby devices do not.

Leakage current is another electric-field-dependent nonideality often present in the SiC MOS-C. This can be attributed to the fact that the electron and hole tunnel barriers are not as high for the SiC/SiO_2 interface as for Si/SiO_2. In addition, the qualities of the oxide and epilayer are not yet as high as in silicon and the pulsed MOS-C measurements require very high temperatures to achieve a reasonable recovery time (400 °C in the present experiments). Gate oxide leakage current extends the MOS-C inversion layer formation time, which can artificially increase the generation lifetimes extracted from the Zerbst plots. The effect of oxide leakage on C-t and Zerbst plots depends on the dependence of the current on oxide electric field, and is explained in detail in [30]. Since it is difficult to obtain accurate generation lifetimes for devices with excessive oxide leakage currents, measurements made on these devices were not considered.

A third electric-field-dependent nonideality that is sometimes present in SiC/SiO_2 MOS-C is mobile ions. Mobile ions can significantly affect the results of the pulsed SiC/SiO_2 MOS-C due to the high temperatures. At 400 °C, typical mobile ions have a very high mobility and quickly drift through the oxide and even the metal gate. Ion motion results in a stretch-out of the capacitance versus time curve near the beginning [Fig. 8(a)], because the field created by their motion offsets the change in electric field in the capacitor due to the generation of the inversion layer. On the Zerbst plot, this typically appears as a flat line or, in extreme cases, as an arc shape [Fig. 8(b)]. The right side of this arc has a negative slope which is interpreted on a Zerbst plot as a negative generation lifetime—clearly indicating an artifact of the measurement. Fortunately, our results indicate that the effect appears to be negligible on the slope of the Zerbst plot close to the origin. This is because most of the ion motion takes place near the beginning of the measurement period, at higher values of the Zerbst axes. Thus, the Zerbst slope should be used near the origin (far from the flat line or arc shape), in order to assure that the generation lifetimes are not affected by ion motion.

An example of the effects of electric-field-dependent nonidealities on the pulsed SiC/SiO_2 MOS-C measurement is shown in Fig. 8. These plots represent a series of seven consecutive pulsed MOS-C measurements. The gate voltages of each run are indicated in the legend. The sequence shows that the behavior as a function of electric field and time under stress is a complicated interdependent relationship which is difficult to deconvolve. However, distinct signatures of certain nonidealities are present. First, "Run 1," in the C-t plot of Fig. 8(a), has a much slower recovery than the subsequent runs. It is also marked by a change in slope at about 6 s. This C-t stretch-out is indicative of the motion of mobile ions returning to the gate, reducing the negative flatband voltage shift. Until this process is complete, the capacitance increase due to the inversion layer generation is offset by the capacitance decrease caused by the flatband voltage shift, which is moving the device further into deep depletion. This behavior is verified by the negative slope on "Run 1" of the Zerbst plot of Fig. 8(b). Subsequent runs at $V_G = -5$ V do not exhibit this behavior. It is also apparent in Fig. 8(a) that the inversion capacitance of the curves tends to be higher for lower voltages (although it also depends on the order in the sequence). This is due to the following effect: A higher gate voltage creates a higher electric field on the gate oxide with the device in inversion. Thus, since gate oxide leakage current is present, the device never completely returns to equilibrium but, instead, a steady-state leakage current balances the generation current. The increase in the steady-state oxide electric field due to a higher gate voltage increases the leakage current. This, in turn, diminishes the steady-state inversion charge and lowers the capacitance. In addition to ion motion and gate leakage, the device in Fig. 8 has a significant increase in generation lifetime with increasing electric field. This can be seen clearly from the Zerbst plot of Fig. 8(c), where the slope near the origin is greatly increased for higher voltages. The lifetimes calculated from this plot are plotted against electric field in Fig. 8(d), showing a strong decrease in generation lifetime with increasing electric field.

Only a small percentage of MOS-C shows the extremely strong electric field dependence of generation lifetime shown in Fig. 8(d). The majority of devices show little correlation between generation lifetime and electric field, as shown in Fig. 9. Furthermore, sometimes, the generation lifetime *increases* with increasing electric field, as in device A3o1-2 in Fig. 9, which is attributed to leakage current extending the recovery time at higher electric fields. Clearly, care must be taken in making these measurements and interpreting the data, since a great deal of variation is possible within one device, depending on the specific measurement conditions.

Authorized licensed use limited to: Arizona State University. Downloaded on August 05,2010 at 17:03:41 UTC from IEEE Xplore. Restrictions apply.

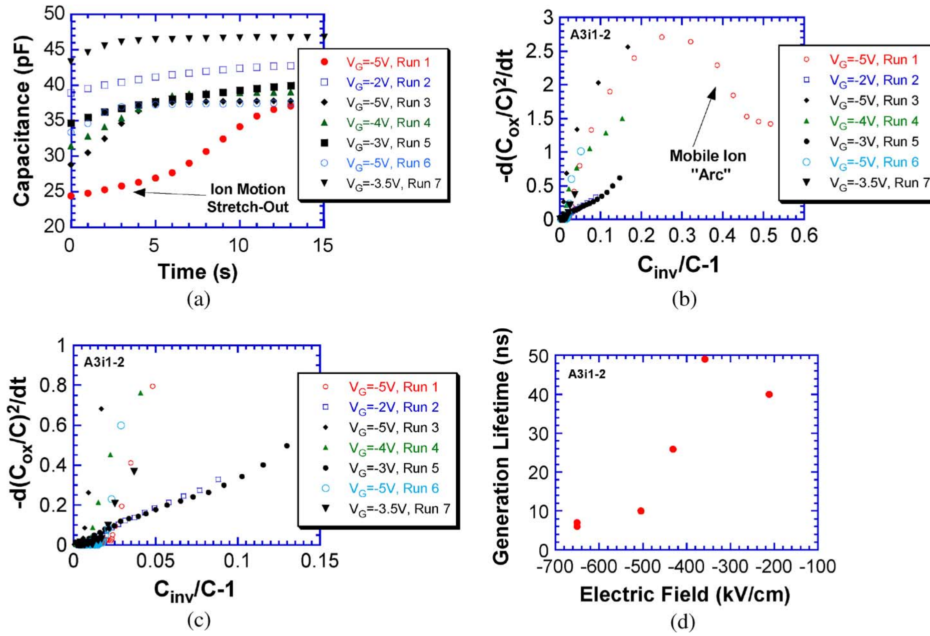

Fig. 8. (a) Experimental C-t data for a MOS-C which represents several field-dependent behaviors with (b) the full corresponding Zerbst plot, (c) a closer view of this Zerbst plot near the origin, and (d) a plot of generation lifetime versus electric field.

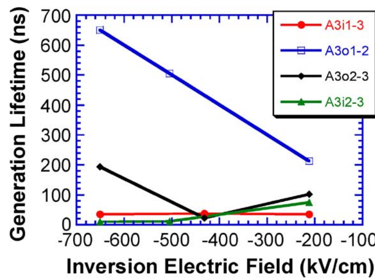

Fig. 9. Generation lifetime versus inversion electric field for several devices discussed in the text.

The presence of surface generation provides a further complication which can skew the interpretation of the Zerbst plot. For reasons explained earlier, when high surface generation is present, it can dominate the generation current, resulting in a value of $\tau_{g,\mathrm{eff}}$ that is much shorter than the generation lifetime in the bulk (SCR). Since the generation lifetimes of the samples reported earlier are effective generation lifetimes, they are subject to this effect. It is possible that these results are simply a measure of the quality of the SiC/SiO_2 interface and do not represent the properties of the underlying epilayer. However, because the intercept of the Zerbst plots generally resulted in low values of $s_{g,\mathrm{eff}}$, it was assumed that the reported values of $\tau_{g,\mathrm{eff}}$ were not dominated by surface generation and do represent the generation lifetimes in the SCR.

It was found that if a MOS-C was subjected to the pulsed generation lifetime measurement several times, the surface generation would increase significantly with each consecutive measurement. This behavior was attributed to NBTI, as described in [29]. To briefly summarize, NBTI is an increase in interface states in a MOS structure due to a negative stress and elevated temperatures [37]. The increased density of interface states causes an increase in surface generation velocity, which increases the Zerbst parameters $s_{g,\mathrm{eff}}$ and decreases $\tau_{g,\mathrm{eff}}$. NBTI is caused by the pulsed MOS-C measurement itself, since for n-type capacitors, it involves negatively biasing the device for several minutes at a high temperature. In the results reported earlier, the effects of NBTI were averted by using low gate voltages and only using the measurement results from a fresh untested device. Therefore, after a device had been measured once, the results of subsequent measurements generally had higher values of $s_{g,\mathrm{eff}}$, and the values of $\tau_{g,\mathrm{eff}}$ were not considered to accurately represent the bulk lifetime.

Unfortunately, NBTI makes it impossible to create an accurate Arrhenius plot for a device, since this involves the repeated measurement of a particular device at various temperatures. The activation energy extracted from such a plot is a function of the measurement sequence and does not indicate the energy level of the dominant generation center. For example, consider Fig. 10. In this case, the pulsed MOS-C was first measured at decreasing temperatures in intervals of 5 °C, starting at 400 °C, and then from 380 °C in increasing intervals back to 400 °C. Fig. 10(a) shows that the effective bulk lifetime is nearly constant with temperature, regardless of the order of the measurements. If this is truly indicative of the bulk lifetime, this plot suggests that the dominant generation center is exactly at E_i. However, the effective surface generation velocity tells a different story, as shown in Fig. 10(b). The surface generation velocity increases at an exponential rate due to the increase in surface states caused by the onset of NBTI. Thus, $s_{g.\mathrm{eff}}$ depends strongly on the order in which the test was run. As noted in (10), $\tau_{g.\mathrm{eff}}$ is affected by surface generation and therefore also depends on the order of the measurement. Hence, the values in Fig. 10(a) most likely do not represent the true bulk lifetimes, and the energy extracted from the Arrhenius plot does not represent the dominant generation center.

This work demonstrates the need for careful interpretation of data resulting from the pulsed MOS-C measurement when applied to the SiC/SiO_2 material system. In order to minimize

Authorized licensed use limited to: Arizona State University. Downloaded on August 05,2010 at 17:03:41 UTC from IEEE Xplore. Restrictions apply.

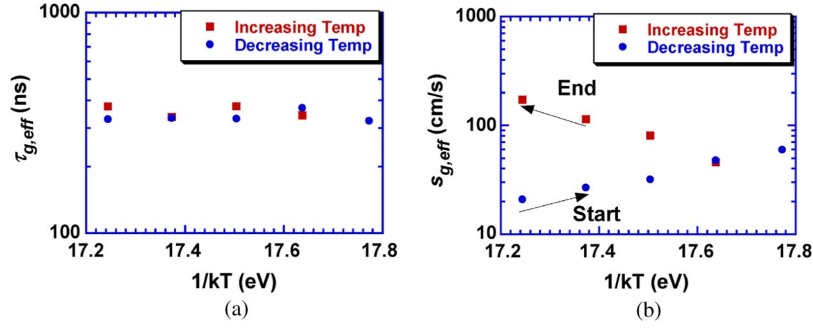

Fig. 10. (a) Arrhenius plot of the effective generation lifetime and (b) the corresponding Arrhenius plot of the effective surface generation velocity.

the effects of leakage current, NBTI, ion motion, and electric-field-enhanced emission, the capacitor should be measured only one time at low gate voltages. Moreover, the device should never be biased in accumulation while at high temperatures. Finally, due to the effects of NBTI, strong caution should be used when interpreting Arrhenius plots obtained from the repeated pulsed MOS-C measurement of the n-type SiC/SiO_2 MOS-C.

D. Recombination Versus Generation Lifetime

A peculiarity arises from the generation and recombination lifetime data presented in the previous sections, as well as that found in the literature. The ratio of generation to recombination lifetimes in SiC is much less than that predicted by theory, or observed experimentally in silicon. From (7), this ratio is

$$\frac{\tau_g}{\tau_r} \approx e^{\frac{|E_T - E_i|}{kT}}. \tag{14}$$

The typical experimental values of τ_g/τ_r in silicon are generally on the order of 50 to 100 [38]. However, our experimental values and all known published results report generation lifetimes ranging from approximately 1 to 1000 ns, whereas the recombination lifetimes are generally on the order of 100 to 5000 ns. The numbers yield values of τ_g/τ_r on the order of 0.001 to 5, which are clearly less than those observed in silicon. Furthermore, (14) predicts that it is not possible to have values of τ_g/τ_r less than unity, as is often the case in SiC. It also indicates that τ_g should correlate with τ_r, which was not observed in the present study—but is generally observed in silicon.

To further examine the possible reasons for these inconsistencies, it is useful to consider what the expected generation and recombination lifetimes should be if they were limited by two bulk point defects. The following analysis is limited to the effects of the $Z1/2$ and $EH6/7$ traps, since they are the levels which are most strongly suspected of limiting carrier lifetimes in 4H-SiC. For low-level injection, the recombination lifetime in an n-type layer is given by the combination of (1) and (4) (ignoring the effects of dislocations and surface recombination)

$$\frac{1}{\tau_r} = \frac{1}{\tau_{p,Z1/2}} + \frac{1}{\tau_{p,EH6/7}}. \tag{15}$$

In terms of defect densities and capture cross sections, (15) is modified to

$$\frac{1}{\tau_r} = \sigma_{p,Z1/2} v_{\rm th} N_{Z1/2} + \sigma_{p,EH6/7} v_{\rm th} N_{EH6/7}. \tag{16}$$

The generation lifetime is given by combining (1) with (5)

$$\frac{1}{\tau_g} = \frac{1}{\tau_{p,Z1/2} e^{\frac{E_T - E_i}{kT}} + \tau_{n,Z1/2} e^{-\frac{E_T - E_i}{kT}}} + \frac{1}{\tau_{p,EH6/7} e^{\frac{E_T - E_i}{kT}} + \tau_{n,EH6/7} e^{-\frac{E_T - E_i}{kT}}}. \tag{17}$$

Equations (16) and (17) allow the calculation of numerical estimates of the recombination and generation lifetimes. Since densities of deep-level impurities and capture cross sections are not available for our data, the numerical results of Klein *et al.* are used to estimate these values [15]. Hence, the densities of $Z1/2$ and $EH6/7$ are assumed to be 2×10^{13} and 1×10^{13} cm^{-3}, respectively. Furthermore, it is assumed that, for $Z1/2$, the capture cross section for electrons is 2×10^{-14} cm^2, and for holes, it is 3.5×10^{-14} cm^2. For $EH6/7$, the capture cross section for electrons is approximately 10^{-13} cm^2, according to Zhang *et al.* [2]. To the best of our knowledge, the $EH6/7$ capture cross section for holes has not been reported. The work of Klein *et al.* [15] concludes that it is negligible, due to the results of p-i-n deep level transient spectroscopy (DLTS) measurements. However, evidence from other DLTS measurements on p-type Schottky diodes has shown that a deep-level trap ($P1$) exists at approximately $E_V + 1.45$ eV with a hole cross section of about $\sigma_p = 10^{-14}$ cm^2 [39], which may be the same carbon vacancy causing $EH6/7$. First, we assume the latter to be true and that $\sigma_{p,EH6/7} = 10^{-14}$ cm^2, and later we discuss the impact of a negligible value of $\sigma_{p,EH6/7}$. For simplicity, $v_{\rm th}$ is assumed to be 10^7 cm/s in the following calculations. Using these data, (16) becomes

$$\tau_r = \left(\sigma_{p,Z1/2} v_{\rm th} N_{Z1/2} + \sigma_{p,EH6/7} v_{\rm th} N_{EH6/7}\right)^{-1} = \left(\frac{1}{140 \text{ ns}} + \frac{1}{1000 \text{ ns}}\right)^{-1} = 125 \text{ ns}. \tag{18}$$

In this case, the recombination lifetime was not influenced very much by the density of $EH6/7$, in agreement with the findings of [15]. Next, consider the generation lifetime. For the $EH6/7$ defect, $E_T - E_i = 0$, and for $Z1/2$, $E_T - E_i \approx 1$ eV. Therefore, (17) becomes

$$\frac{1}{\tau_g} = \frac{1}{\tau_{p,Z1/2} e^{\frac{E_T - E_i}{kT}} + \tau_{n,Z1/2} e^{-\frac{E_T - E_i}{kT}}} + \frac{1}{\tau_{p,EH6/7} + \tau_{n,EH6/7}}. \tag{19}$$

Authorized licensed use limited to: Arizona State University. Downloaded on August 05,2010 at 17:03:41 UTC from IEEE Xplore. Restrictions apply.

At a temperature of 400 °C, the $(E_T - E_i)/kT$ term is approximately 17, and (19) reduces further to

$$\tau_g = \left(\frac{1}{\tau_{p,Z1/2}e^{17} + \tau_{n,Z1/2}e^{-17}} + \frac{1}{\tau_{p,EH6/7} + \tau_{n,EH6/7}}\right)^{-1} = \left(\frac{1}{4.2 \times 10^9 \text{ ns}} + \frac{1}{1000 \text{ ns} + 100 \text{ ns}}\right)^{-1} \approx 1100 \text{ ns} \quad (20)$$

Consequently, in this example, the lifetime is mainly determined by the $EH6/7$ hole emission time because the contribution of the $Z1/2$ defect to the generation defect is negligible due to its energy from the center of the bandgap.

This analysis demonstrates the following concept: Recombination lifetime can be limited by several defects, but in most cases, generation lifetime is limited by the defect with the energy closest to E_i. In the case of 4H-SiC, this is the $EH6/7$ center. For the $Z1/2$ to affect the generation lifetime at 400 °C, the product $\sigma_{p,Z1/2}N_{Z1/2}$ would have to be 3×10^7 times smaller than that of the $EH6/7$ level. At 25 °C, this ratio is approximately 10^{17}. Thus, even though the $Z1/2$ defect appears to limit the *recombination* lifetime in n-type material, it is nearly impossible for it to limit the *generation* lifetime when the $EH6/7$ defect is present. It should be noted that the $P1$ hole trap has not been extensively studied, and it is possible that it is caused by a different physical mechanism than that which causes the $EH6/7$. Very limited DLTS measurements and recombination lifetime data are available for p-type 4H-SiC compared to n-type; for this reason, the cross section for holes for the $EH6/7$ is not known with certainty. Thus, we now consider the generation lifetime if the $\sigma_{\text{pEH6/7}} = 10^{-17}$ cm^2, as specified in [1]. In this case, (17) becomes

$$\tau_g = \left(\frac{1}{3 \times 10^7 \tau_{p,Z1/2}} + \frac{1}{\tau_{p,EH6/7} + \tau_{n,EH6/7}}\right)^{-1} = \left(\frac{1}{4.2 \times 10^9 \text{ ns}} + \frac{1}{10^6 + 100 \text{ ns}}\right)^{-1} = 1 \text{ ms}. \quad (21)$$

The nearness of the $EH6/7$ energy level to E_i still causes it to dominate the generation lifetime, but the very slow hole emission predicts the long lifetime of 1 ms. However, generation lifetimes in excess of a few microseconds have never been observed in 4H-SiC. Thus, if the hole capture cross section of the $EH6/7$ defect is this small, then the short generation lifetimes must be due to defects other than bulk traps. Moreover, the fact that the τ_g/τ_r ratio is usually near or less than unity suggests that the deep level dominating the generation lifetime must be near the center of the bandgap. Given the known densities and capture cross sections of traps, it is highly unlikely that a deep level further than a few hundreds of millielectronvolts from the center of the band plays *any* significant role in the generation lifetime.

It is difficult to accurately extend these theoretical considerations to surface generation over a continuum of interface trap states. While the D_{it} measurements for the aforementioned samples give densities less than 5×10^{11} eV^{-1}cm^{-2} at 200 meV from the conduction band, the D_{it} levels near E_i are not known. In addition, there are no published reports of the capture cross sections of surface traps (σ_s) for the 4H-SiC/SiO_2 interface. A detailed experimental study of D_{it} and σ_s across all energies for the 4H-SiC/SiO_2 would allow an accurate quantitative analysis of surface generation and is a worthwhile future effort.

Despite the lack of the necessary data to quantify the surface generation, it is known that the SiC/SiO_2 interface always has a high D_{it} (compared to modern Si/SiO_2 levels), and it might seem logical to conclude that all of the generation lifetimes ever measured on 4H and 6H-SiC are dominated by surface generation rather than bulk point defects. While this is possible, we do not believe this to be the case. Even though D_{it} is often very high near the band edges, densities of deeper states are usually lower. As with bulk generation, deep states near the band center are the most efficient in the emission process and thus have the greatest effect on surface generation.

Furthermore, the intercept of the Zerbst plot used to provide generation lifetime data in the present work provides an estimate of the MOS-C surface generation velocity. Generally, a virgin device exhibited a low surface generation velocity—usually less than 30 cm/s. Subsequent measurements always show a precipitous increase in the Zerbst intercept, indicating an increase in $s_{g,\text{eff}}$ to several hundreds of centimeters per second, as the density of interface states increases due to NBTI. This behavior indicates that the intercept of the Zerbst plot is a reasonable indication of surface generation velocity and that most of the devices had a low surface generation during the initial pulsed MOS-C measurement. This suggests that bulk generation lifetimes in the present samples truly are on the order of 1 ns to 1 μs.

Additional evidence that the low generation lifetimes observed in SiC are not exclusively caused by surface generation is given by Wang *et al.* [28]. In this paper, an n-p-n capacitor is used, which is less prone to surface effects than a standard MOS-C. Nonetheless, many of the n-p-n capacitors still exhibited strong surface generation through the surfaces of the oxide sidewall. The authors of this paper proceeded to systematically study devices of various perimeter-to-area ratios. These results were used to separate the surface and bulk components of the generation current. The results gave *bulk* generation lifetimes of about 50 ns, which is on the order of those presented in this paper, as well as in the literature. Thus, it is reasonable to conclude that surface generation is not the only factor limiting generation lifetimes in this work.

Several other factors might be responsible for the abnormal relationship between recombination and generation lifetimes. Most recombination lifetime data are provided from optical measurements. Optical measurements yield an average recombination lifetime over the optical penetration depth, which is about 50 μm for the 355-nm laser used in the current work [1]. On the other hand, the pulsed MOS-C measurements are only influenced by the volume within the SCR, which extends only about 1 μm below the SiC/SiO_2 interface. As a result, high defect densities very close to the SiC/SiO_2 interface (but not necessarily at the interface) would reduce the generation

Authorized licensed use limited to: Arizona State University. Downloaded on August 05,2010 at 17:03:41 UTC from IEEE Xplore. Restrictions apply.

lifetimes much more than the corresponding recombination lifetimes. In addition, generation lifetime is defined as $\tau_g \equiv n_i/G$, and therefore, an inaccuracy in the intrinsic carrier concentration is directly reflected in the generation lifetime. If the value of n_i used in our calculations (1.8×10^8 cm^{-3} at 400 °C) is lower than the real value, the calculated generation lifetimes would be proportionally lower than the real values.

At this time, it is difficult to determine which defect limits the generation lifetime when dislocations are below the threshold density of about 10^6 cm^{-2}. It is also debatable which defects limit recombination lifetimes, but current results indicate that it is the $Z1/2$ or $EH6/7$ defects. It is reasonable to conclude that $Z1/2$ defect cannot affect the generation lifetime in current 4H-SiC materials due to the large distance of the corresponding energy level from E_i. If the $Z1/2$ is responsible for limiting the recombination lifetime, then the generation and recombination lifetimes in SiC do not depend on the same defect. In the case where the ratio τ_g/τ_r is close to unity, then the generation lifetime could be limited by a point defect with an energy level close to E_i, such as the $EH6/7$ defect—but only if $\sigma_{p,\mathrm{EH6/7}}$ has an cross-sectional area of at least 10^{-14} cm^2. When τ_g/τ_r is much less than unity (i.e., $\tau_g < 10$ ns), it is impossible that the τ_g is limited by emission through a single-level point defect. In this case, τ_g may be limited by field-enhanced emission through traps near the surface; it is also possible that charge is transported to the SCR through decorated dislocations. Hence, it can be concluded that the generation lifetimes of MOS-C in a small area (less than 1 cm^2) are limited by several different factors—possibly none of which affects the recombination lifetimes. Further comparison of the macroscopic generation lifetimes with microscopic material properties of the epilayer and oxide/epilayer interface is necessary to fully understand the phenomenon limiting the generation lifetimes in the pulsed SiC MOS-C.

VI. Conclusion

For the first time, generation lifetimes, dislocation densities, recombination lifetimes, and Schottky diode characteristics have been analyzed for the same location on SiC samples. Generation lifetimes appear to be limited by dislocations at densities higher than 10^6 cm^{-2} and are similar for samples with epilayers grown at 4° and 8°. Very low Schottky barrier heights correspond to shorter generation lifetimes on average, but there were some individual devices which contradicted this behavior. The ratio of τ_g/τ_r in SiC is much less than that observed in silicon. Generation lifetime cannot be limited by the $Z1/2$ defect, but might be limited by the $EH6/7$ defect in cases where τ_g/τ_r is near unity. In cases where this ratio is much less than unity, it is hypothesized that the generation lifetime is limited by electric-field-enhanced emission near the surface or charge transport through decorated dislocations. Understanding the nature of generation lifetime in SiC, as well as the defects near the surface of the SiC/SiO_2 MOS-C, should be considered a worthwhile subject of ongoing investigations, as it may eventually catalyze the development of a high-quality commercial SiC MOSFET.

References

[1] P. B. Klein, "Carrier lifetime measurement in n- 4H-SiC epilayers," *J. Appl. Phys.*, vol. 103, no. 33, pp. 033 702-1–033 702-14, Feb. 2008.

[2] J. Zhang, L. Storasta, J. P. Bergman, N. T. Son, and E. Janzen, "Electrically active defects in n-type 4H-silicon carbide grown in a vertical hot-wall reactor," *J. Appl. Phys.*, vol. 93, no. 8, pp. 4708–4714, Apr. 2003.

[3] R. F. Pierret, *Advanced Semiconductor Fundamentals*, 2nd ed. Upper Saddle River, NJ: Pearson Education, 2003.

[4] D. K. Schroder, *Semiconductor Material and Device Characterization*, 3rd ed. Hoboken, NJ: Wiley, 2006.

[5] C. T. Sah, "The equivalent circuit model in solid-state electronics—Part I: The single energy level defect centers," *Proc. IEEE*, vol. 55, no. 5, pp. 654–671, May 1967.

[6] W. Shockley and W. T. Read, "Statistics of the recombination of holes and electrons," *Phys. Rev.*, vol. 87, no. 5, pp. 835–842, Sep. 1952.

[7] R. N. Hall, "Electron-hole recombination in germanium," *Phys. Rev.*, vol. 87, no. 2, p. 387, Jul. 1952.

[8] D. K. Schroder, "Carrier lifetimes in silicon," *IEEE Trans. Electron Devices*, vol. ED-44, no. 1, pp. 160–170, Jan. 1997.

[9] A. S. Grove and D. J. Fitzgerald, "Surface effects on pn junctions: Characteristics of surface space-charge regions under nonequilibrium conditions," *Solid State Electron.*, vol. 9, no. 8, pp. 783–806, Aug. 1966.

[10] S. R. Morrison, "Recombination of electrons and holes at dislocations," *Phys. Rev.*, vol. 104, no. 3, pp. 619–623, Nov. 1956.

[11] W. T. Read, "Theory of dislocations in germanium," *Philos. Mag.*, vol. 45, no. 367, pp. 775–796, 1954.

[12] J. P. McKelvey, "Experimental determination of injected carrier recombination rates at dislocations in semiconductors," *Phys. Rev.*, vol. 106, no. 5, pp. 910–917, Jun. 1957.

[13] G. K. Wertheim and G. L. Pearson, "Recombination in plastically deformed germanium," *Phys. Rev.*, vol. 107, no. 3, pp. 694–698, Aug. 1957.

[14] S. Nigam, "Carrier lifetimes in silicon carbide," Ph.D. dissertation, Carnegie Melon Univ., Pittsburgh, PA, Mar., 2008.

[15] P. B. Klein, B. V. Shanabrook, S. W. Huh, A. Y. Polyakov, M. Skowronski, J. J. Sumakeris, and M. J. O'Loughlin, "Lifetime-limiting defects in n(-) 4H-SiC epilayers," *Appl. Phys. Lett.*, vol. 88, no. 5, pp. 052 110-1–052 110-3, Jan. 2006.

[16] C. Hemmingsson, N. T. Son, O. Kordina, J. P. Bergman, E. Janzen, J. L. Lindstrom, S. Savage, and N. Nordell, "Deep level defects in electron-irradiated 4H-SiC epitaxial layers," *J. Appl. Phys.*, vol. 81, no. 9, pp. 6155–6159, May 1997.

[17] O. Kordina, J. P. Bergman, C. Hallin, and E. Janzen, "The minority carrier lifetime of n-type 4H- and 6H-SiC epitaxial layers," *Appl. Phys. Lett.*, vol. 69, no. 5, pp. 679–681, Jul. 1996.

[18] T. Tawara, H. Tsuchida, S. Izumi, I. Kamata, and K. Izumi, "Evaluation of free carrier lifetime and deep levels of the thick 4H-SiC epilayers," *Mater. Sci. Forum*, vol. 457, pp. 565–568, 2004.

[19] K. Danno, D. Nakamura, and T. Kimoto, "Investigation of carrier lifetime in 4H-SiC epilayers and lifetime control by electron irradiation," *Appl. Phys. Lett.*, vol. 90, no. 20, pp. 202 109-1–202 109-3, May 2007.

[20] A. Galeckas, J. Linnros, M. Frischholz, and V. Grivickas, "Optical characterization of excess carrier lifetime and surface recombination in 4H/6H-SiC," *Appl. Phys. Lett.*, vol. 79, no. 3, pp. 365–367, Jul. 2001.

[21] G. Y. Chung, M. J. Loboda, M. J. Marinella, D. K. Schroder, P. B. Klein, T. Isaacs-Smith, and J. W. Williams, "Generation and recombination carrier lifetimes in 4H SiC epitaxial wafers," *Mater. Sci. Forum*, vol. 90, pp. 556–557, 2007.

[22] T. Mori, M. Kato, H. Watanabe, M. Ichimura, E. Arai, S. Sumie, and H. Hashizume, "Excess carrier lifetime measurement of bulk SiC wafers and its relationship with structural defect distribution," *Jpn. J. Appl. Phys. 1, Reg. Papers Brief Commun. Review Papers*, vol. 44, no. 12, pp. 8333–8339, Dec. 2005.

[23] T. Kimoto, N. Miyamoto, and H. Matsunami, "Performance limiting surface defects in SiC epitaxial p-n junction diodes," *IEEE Trans. Electron Devices*, vol. 46, no. 3, pp. 471–477, Mar. 1999.

[24] C. J. Cochrane, P. M. Lenahan, and A. J. Lelis, "Deep level defects which limit current gain in 4H SiC bipolar junction transistors," *Appl. Phys. Lett.*, vol. 90, no. 12, pp. 123 501-1–123 501-3, Mar. 2007.

[25] J. R. Jenny, D. P. Malta, V. F. Tsvetkov, M. K. Das, H. M. Hobgood, C. H. Carter, R. J. Kumar, J. M. Borrego, R. J. Gutmann, and R. Aavikko, "Effects of annealing on carrier lifetime in 4H-SiC," *J. Appl. Phys.*, vol. 100, no. 11, pp. 113 710-1–113 710-3, Dec. 2006.

[26] P. Neudeck, S. Kang, J. Petit, and M. Tabibazar, "Measurement of n-type dry thermally oxidized 6H-SiC metal–oxide–semiconductor diodes by quasi-static and high-frequency capacitance versus voltage and capacitance transient techniques," *J. Appl. Phys.*, vol. 75, no. 12, pp. 7949–7953, Jun. 1994.

Authorized licensed use limited to: Arizona State University. Downloaded on August 05,2010 at 17:03:41 UTC from IEEE Xplore. Restrictions apply.

[27] J. N. Pan, J. A. Cooper, and M. R. Melloch, "Extremely long capacitance transients in 6H-SiC metal–oxide–semiconductor capacitors," *J. Appl. Phys.*, vol. 78, no. 1, pp. 572–574, Jul. 1995.

[28] Y. Wang, J. A. Cooper, M. R. Melloch, S. T. Sheppard, J. W. Palmour, and L. A. Lipkin, "Experimental characterization of electron-hole generation in silicon carbide," *J. Electron. Mater.*, vol. 25, no. 5, pp. 899–907, May 1996.

[29] M. J. Marinella, D. K. Schroder, T. Isaacs-Smith, A. C. Ahyi, J. R. Williams, G. Y. Chung, J. W. Wan, and M. J. Loboda, "Evidence of negative bias temperature instability in 4H-SiC metal oxide semiconductor capacitors," *Appl. Phys. Lett.*, vol. 90, no. 25, pp. 253 508-1–253 508-3, Jun. 2007.

[30] M. J. Marinella, D. K. Schroder, T. Isaacs-Smith, J. R. Williams, G. Y. Chung, and M. J. Loboda, "A "probe-lift" MOS-capacitor technique for measuring very low oxide leakage currents and their effect on generation lifetime extraction," *IEEE Trans. Electron Devices*, vol. 55, no. 2, pp. 565–571, Feb. 2008.

[31] Y. Wang, G. N. Ali, M. K. Mikhov, V. Vaidyanathan, B. J. Skromme, B. Raghothamachar, and M. Dudley, "Correlation between morphological defects, electron beam-induced current imaging, and the electrical properties of 4H-SiC Schottky diodes," *J. Appl. Phys.*, vol. 97, no. 1, pp. 013 540-1–013 540-10, Jan. 2005.

[32] B. J. Skromme, E. Luckowski, K. Moore, M. Bhatnagar, C. E. Weitzel, T. Gehoski, and D. Ganser, "Electrical characteristics of Schottky barriers on 4H-SiC: The effects of barrier height nonuniformity," *J. Electron. Mater.*, vol. 29, no. 3, pp. 376–383, Mar. 2000.

[33] D. J. Ewing, L. M. Porter, Q. Wahab, X. Ma, T. S. Sudharshan, S. Tumakha, M. Gao, and L. J. Brillson, "Inhomogeneities in Ni/4H-SiC Schottky barriers: Localized Fermi-level pinning by defect states," *J. Appl. Phys.*, vol. 101, no. 11, pp. 114 514-1–114 514-10, Jun. 2007.

[34] K. B. Park, Y. Ding, J. P. Pelz, M. K. Mikhov, Y. Wang, and B. J. Skromme, "Effect of inclined quantum wells on macroscopic capacitance–voltage response of Schottky contacts: Cubic inclusions in hexagonal SiC," *Appl. Phys. Lett.*, vol. 86, no. 22, pp. 222 109-1–222 109-3, May 2005.

[35] B. J. Skromme, K. Palle, C. D. Poweleit, L. R. Bryant, W. M. Vetter, M. Dudley, K. Moore, and T. Gehoski, "Oxidation-induced crystallographic transformation in heavily N-doped 4H-SiC wafers," *Mater. Sci. Forum*, vol. 389–393, pp. 455–458, 2002.

[36] P. U. Calzolari, S. Graffi, and C. Morandi, "Field-enhanced carrier generation in MOS capacitors," *Solid State Electron.*, vol. 17, no. 10, pp. 1001–1011, Oct. 1974.

[37] D. K. Schroder, "Negative bias temperature instability: What do we understand?," *Microelectron. Reliab.*, vol. 47, no. 6, pp. 841–852, Jun. 2007.

[38] D. K. Schroder, "The concept of generation and recombination lifetimes in semiconductors," *IEEE Trans. Electron Devices*, vol. ED-29, no. 8, pp. 1336–1338, Aug. 1982.

[39] K. Danno, T. Kimoto, and H. Matsunami, "Midgap levels in both n- and p-type 4H-SiC epilayers investigated by deep level transient spectroscopy," *Appl. Phys. Lett.*, vol. 86, no. 12, pp. 122 104-1–122 104-3, Mar. 2005.

Matthew J. Marinella (S'03–M'08) was born in Arizona in 1981. He received the B.S.E. and Ph.D. degrees in electrical engineering from Arizona State University, Tempe, in 2004 and 2008, respectively.

From 2008 to 2010, he was a Device Engineer with Microchip Technology in Tempe. Since March 2010, he has been with Sandia National Laboratories, Albuquerque, NM, as a Senior Member of the Technical Staff in the Radiation Hardened CMOS Technology Department. His research interests include semiconductor device physics and characterization.

Dieter K. Schroder (S'61–M'67–SM'78–F'86–LF'01) received the B.S. and M.S. degrees in electrical engineering from McGill University, Montreal, QC, Canada, in 1962 and 1964, respectively, and the Ph.D. degree in electrical engineering from the University of Illinois, Chicago, in 1968.

In 1968, he joined the Westinghouse Research Laboratories, where he was engaged in research on various aspects of semiconductor devices, including MOS devices, imaging arrays, power devices, and magnetostatic waves. He spent a year at the Institute of Applied Solid State Physics in Germany during 1978. Since 1981, he has been with the Center for Solid State Electronics Research, Arizona State University, Tempe. He has written the books *Advanced MOS Devices* and *Semiconductor Material and Device Characterization*, has published over 170 papers, supervised 105 graduate students, and is the holder of five patents. His current interests are semiconductor materials and devices, characterization, low-power electronics, and defects in semiconductors.

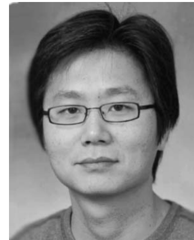

Gilyong Chung received the B.S. degree in ceramic engineering from Yonsei University, Seoul, Korea, in 1990 and the Ph.D. degree in electronic materials engineering from the Korea Advanced Institute of Science and Technology, Daejeon, Korea, in 1995, where he worked on thin-film CdS/CdTe solar cell fabrication and characterization.

He was with Samsung SDI as a Project Leader to develop new LED devices with Si materials. After two years as a Research Associate working on SiC MOSFET developments at Auburn University, Auburn, AL, he joined Sterling Semiconductor Inc. as a Senior Device Engineer in 2001 and was responsible for the research and development activities of SiC rectifiers and MOS interface optimization. He is currently with Dow Corning Compound Semiconductor Solutions, LLC, Midland, MI, working on various metrologies for SiC materials and investigating correlation between SiC material defects and device performance. He has coauthored over 60 publications in various conference proceedings and refereed journals and is an inventor on three issued U.S. patents.

Mark J. Loboda (M'87–SM'98) received the B.S. and M.S. degrees (with honors) in applied physics, with emphasis in the areas of solid-state physics, electronics, and nuclear magnetic resonance spectroscopy, from DePaul University, Chicago, IL, in 1983 and 1985, respectively.

From 1985 to 1989, he was a Staff Scientist with the Research Division, Raytheon Company, Lexington, MA, where he performed basic research on high-Q resonator structures and low-noise RF/microwave oscillator technology focusing on surface acoustic wave devices, high-permittivity materials, and superconductors. In 1989, he joined the Dow Corning Corporation, Midland, MI. At Dow Corning, he established research programs in the areas of thin-film characterization, thin-film deposition (PECVD/CVD), CVD precursor development, and semiconductor device fabrication. He is an internationally recognized authority in the area of low-permittivity dielectric materials and applications. In 2002, he was named a Dow Corning Research Scientist. He is currently the Science and Technology Leader with Dow Corning Compound Semiconductor Solutions, LLC, Midland. He has published over 50 technical papers and has been awarded numerous patents in areas such as RF and microwave electronics, silicon alloys, low-permittivity dielectric materials, electrical and optical spectroscopy, and chemical vapor deposition. His current research interests focus on the growth and characterization of silicon carbide semiconductors.

Authorized licensed use limited to: Arizona State University. Downloaded on August 05,2010 at 17:03:41 UTC from IEEE Xplore. Restrictions apply.

Tamara Isaacs-Smith received the B.A. degree in chemical physics from Bryn Mawr College, Bryn Mawr, PA, in 1985 and the M.S. degree in chemical physics from the University of Maryland, College Park, in 1988.

From 1989 to 1991, she was a Physicist with Tad Technical Services and, from 1991 to 1993, a Development Editor with the Institute of Physics. Since 1994, she has been a Senior Research Associate with the Physics Department, Auburn University, Auburn, AL. Her research concentrates on the study of SiC, particularly in developing devices.

John R. Williams (S'83–M'83) received the Ph.D. degree in physics from North Carolina State University, Raliegh.

Since 1974, he has been with the Physics Department, Auburn University, Auburn, AL, where he is currently a Thomas and Jean Walter Professor. His research interests include electrical characterization of wide bandgap semiconductor materials, WBG device fabrication and characterization, and research applications for megaelectronvolt ion accelerators—particularly those that support semiconductor material modification and analysis using the techniques of heavy ion implantation, Rutherford backscattering spectrometry, light ion channeling, and nuclear reaction analysis.

Dr. Williams is a member of the American Physical Society and the Materials Research Society.

Authorized licensed use limited to: Arizona State University. Downloaded on August 05,2010 at 17:03:41 UTC from IEEE Xplore. Restrictions apply.